Send Orders for Reprints to reprints@benthamscience.ae

Current Pharmaceutical Biotechnology, 2016, *17*, 000-000

Controlled Drug Delivery Using Microdevices

Sharma T. Sanjay[1], Maowei Dou[1], Guanglei Fu[1], Feng Xu[2] and XiuJun Li[1,3,4*]

[1]*Department of Chemistry, University of Texas at El Paso, 500 West University Ave, El Paso, Texas 79968, USA;* [2]*Bioinspired Engineering and Biomechanics Center (BEBC), Xi'an Jiaotong University, Xi'an 710049, P.R. China;* [3]*Biomedical Engineering, University of Texas at El Paso, 500 West University Ave, El Paso, Texas 79968, USA;* [4]*Border Biomedical Research Center, University of Texas at El Paso, 500 West University Ave, El Paso, Texas 79968, USA*

X. Li

Abstract: Therapeutic drugs administered systematically are evenly distributed to the whole body through blood circulation and have to cross many biological barriers before reaching the pathological site. Conventional drug delivery may make drugs inactive or reduce their potency as they may be hydrolyzed or degraded enzymatically and are rapidly excreted through the urinary system resulting in suboptimal concentration of drugs at the desired site. Controlled drug delivery aims to localize the pharmacological activity of the drug to the desired site at desired release rates. The advances made by micro/nanofluidic technologies have provided new opportunities for better-controlled drug delivery. Various components of a drug delivery system can be integrated within a single tiny micro/nanofluidic chip. This article reviews recent advances of controlled drug delivery made by microfluidic/nanofluidic technologies. We first discuss microreservoir-based drug delivery systems. Then we highlight different kinds of microneedles used for controlled drug delivery, followed with a brief discussion about the current limitations and the future prospects of controlled drug delivery systems.

Keywords: Controlled/targeted drug delivery, pharmacological activity, micro/nanofluidic technologies, microdevices, microreservoir, and microneedle.

1. INTRODUCTION

A drug delivery system plays a vital role in controlling various processes of drug administration such as absorption, distribution and elimination, either by immediately releasing the drug or lengthening the release from days to months. Therapeutic drugs that are administered systematically are distributed to the whole body through blood circulation and can also be hydrolyzed or degraded enzymatically and rapidly excreted through the urinary system, resulting in suboptimal concentration of drugs at the desired site. Controlled and targeted drug delivery improves the bio-distribution of a drug, increases the circulation half-life and also protects the drug from the microenvironment, to increase the efficiency and reduce related side effects. The ultimate goal of the drug delivery system is to deliver drugs to the target site and release drugs at a desired rate [1, 2].

1.1. Conventional Drug Delivery and Its Limitations

Conventional drug delivery methods administer therapeutic compound through mouth, trans-mucosal area, skin, inhalation or injection. One of the major challenges of these conventional drug delivery systems is that it is difficult to achieve targeted and effective administration. Most of the drugs, which are in the clinical phase, do not give reassuring results as they fail to reach the destined site of action [3]. Most of the therapeutic drugs do not concentrate selectively in the targeted cells, tissues or organs but are evenly distributed throughout the body and have to cross many biological barriers before reaching pathological sites of action and may get inactivated on their way. Different new drugs including DNA-based therapeutics, proteins and peptides are more susceptible to enzymatic degradation; conventional drug delivery may make the drug inactive or reduce its potency. In addition, the drug may become less effective, as the effective concentration of the drug is lowered at the site of action [4]. Hence, drugs may have to be used in higher quantity, which not only increases the cost of treatment, but also may cause undesirable effect to normal cells and tissues in the body, especially when the therapeutic drugs are cytotoxic. Additionally, there is burst release of a therapeutic drug in conventional methods, which not only reduces the efficacy of the therapy but also increases the risk of side effects and toxicity. Finally, low affinity between drugs and pathological sites may decrease the desired action of the therapeutic drug [5]. These conventional drug delivery methods are often confronted with limitations due to a drug's poor solubility and aggregation, high toxicity, non-specific delivery and high dosage.

Drug delivery and release with the subsequent therapeutic efficacy depends upon several factors including route of application, mechanism of release, particle size, and delivery

*Address correspondence to this author at the Department of Chemistry, Faculty of University of Texas at El Paso, 500 West University Ave, El Paso, Texas 79968, USA; Tel: +1-915-747-8967; E-mail: xli4@utep.edu

1389-2010/16 $58.00+.00

and targeting methods [6]. Sethi *et al.* demonstrated that drug release kinetics could affect the therapeutic efficacy of nanoparticle (NP) docetaxel (DTX) and wortmannin both *in vitro* and *in vivo,* where hepatotoxicity decreased with decrease in drug release kinetics [7]. In the immediate release profile or the conventional drug release there is a sudden burst release of the drug after the administration where the drug concentration might reach the toxic range, followed by a sharp decrease in the concentration of the drug reaching the sub-therapeutic range after a short duration of time. The optimum drug concentration lasts only for a short period of time, minimizing the therapeutic efficacy (Fig. **1A**). The effectiveness of these conventional drugs is also limited by the side effect and their toxicity when the drug concentration reaches the toxic range. Sustained release of the drug is desired as the release of the drug in this case is within the therapeutic range, although the drug concentration might decrease with the time. With the controlled release of a drug, drug concentration can be sustained within the therapeutic window over a long period of time (Fig. **1B**), increasing therapeutic efficacy as well as patient compliance. It helps to minimize local and systemic side effects of the drug and improves bioavailability of the drug. Sustained release provides a promising way to decrease side effect by preventing fluctuation of the therapeutic concentration of drugs in the body as they are designed to release drugs at a predetermined rate in order to maintain constant drug concentration for a specific period of time [8]. An ideal condition would be the zero-order kinetics for the release of the drug where the release of the drug is within the therapeutic range (Fig. **1B**), maximizing the therapeutic efficacy. For some specific drugs like insulin and hormones it is desired to have a pulsatile release of the drug to mimic the natural pulsatile release as in human body. Diseases including peptic ulcer, asthma, arthritis, and diabetes where rhythmic circadian organization of the body plays an important role and the pharmacokinetics is not constant within 24 hr usually require pulsatile release of the drug [9]. There are several studies for the controlled pulsatile release of drugs [10,11].

1.2. Microtechnology for Controlled Drug Delivery

Microtechnology for drug delivery can be described as the fabrication or assembly of different constituents that develop into a drug delivery system with its facets in the micro-scale. These microdevices have their channels/reservoirs in micro-scale while the overall dimension of the devices may be few square millimeters/centimeters. The advances made in the field of micro/nanotechnologies have made it possible to shorten the delivery pathway and make it highly targeted. Now, due to the miniaturization made by the micro/nanotechnologies, it is also possible to integrate various components of the drug delivery system within a single micro/nanofluidic chip. These microdevices can be either implanted within the body in specific tissues/organs, given orally or may be applied externally through the skin. Since the microfluidic lab-on-a-chip (LOC) device is small and more compacted [12-16], it has advantages including ease of use, reduced pain, portability and improved safety. Drug delivery systems based on LOC technologies are advanced enough to administer the controlled amount of therapeutic drugs in a continuous manner. In addition, both the synthesis and delivery of drugs may be integrated into a single device [17, 18].

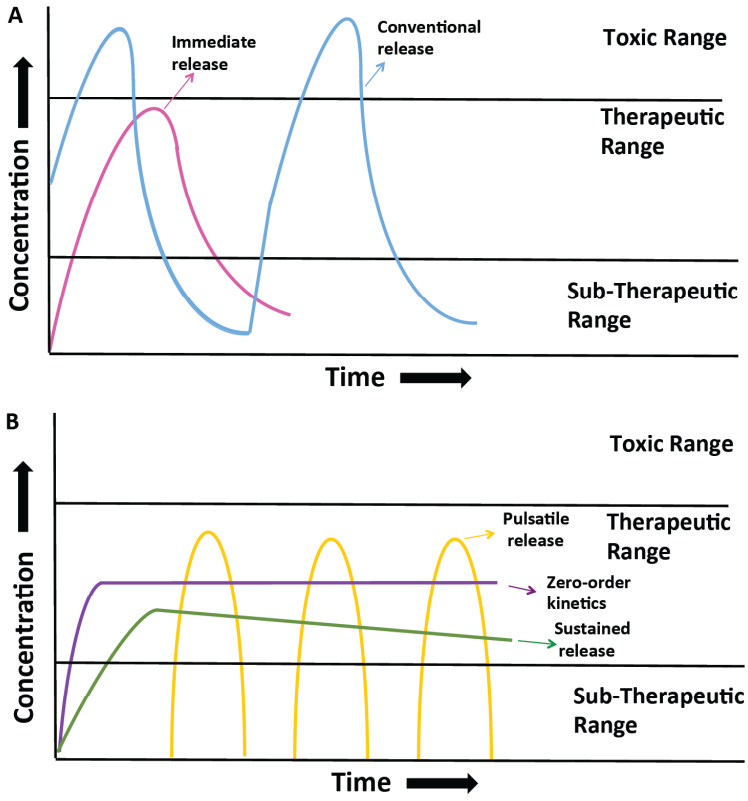

Fig. (1). Drug release profiles. (**A**) Conventional and immediate release. (**B**) Pulsatile, zero-order, and sustained drug release.

Hence, after a brief introduction of microfabrication technologies, this article reviews recent advances of controlled drug delivery systems using microtechnologies, which can be categorized into microreservoir and microneedle (MN)-based delivery systems based on the shape of the drug delivery microstructures and modes of application. Microreservoir-based drug delivery systems include silicon and polymer-based devices, while MNs cover different kinds of MNs including solid, hollow, coated, dissolvable, and porous MNs. Other nanoparticle-based drug delivery systems and applications have been reviewed in a few other articles [19-23].

2. MICROFLUIDIC FABRICATION

Microfluidic LOC, one of the booming technologies with potential to significantly transform engineering, chemistry, and bio-health science field has attracted intensive interest in diverse fields including particle synthesis [24], drug discovery [25], disease diagnostics and biosensors [26-28], drug and gene delivery [21, 29-31], single cell analysis [32-34], and single molecule detection [35]. Microdevices for the delivery of drugs are usually fabricated with polymers or silicon. Photolithography, etching and deposition steps from standard microelectromechanical systems (MEMS) manufacturing technologies are usually followed to fabricate these microfluidic devices or reservoir and MN-based devices [2, 36, 37]. Although photolithography is one of the most widely used techniques, replica molding and surface machining technique are also used to fabricate these devices. Nanofluidic devices have also been used to deliver drugs, but these devices need cleanroom for fabrication and use techniques such as bulk nanomachining, surface nanomachining, buried channel technology, and nanoimprinted lithography [2]. In addition, laser micromachining is one of the non-contact single-step method to fabricate polymeric materials for drug delivery application. Different kinds of lasers have been used for microfabrication including ultra-violet (UV) lasers, pulsed CO_2 lasers, and solid-state femtosecond lasers [38-41]. MNs have been fabricated using technologies including photolithography, micromoulding, droplet-born air blowing (DAB), and layer-by-layer (LbL) assembly [42-46]. Since the focus of this article is not to review microfabrication technologies, we will briefly introduce the photolithography technique in the following paragraph. Details of different microfabrication techniques can be found in the book entitled "Microfluidic Devices for Biomedical Applications" [2].

Figure **2** shows the schematic of a typical SU-8 photolithography process. Drawing of the pattern to be created is first transferred to a photomask or a transparency film. A silicon wafer is taken and treated with photoresist then exposed to UV light through the photomask to create a positive relief of photoresist on a silicon wafer (master). Replica molding is then performed to form microstructures in the polymer once a pre-polymer is poured in the master mold and solidified. The polymeric structure is then peeled off. The cured polymer replica can be bonded to another layer of polymer or glass to form a closed system.

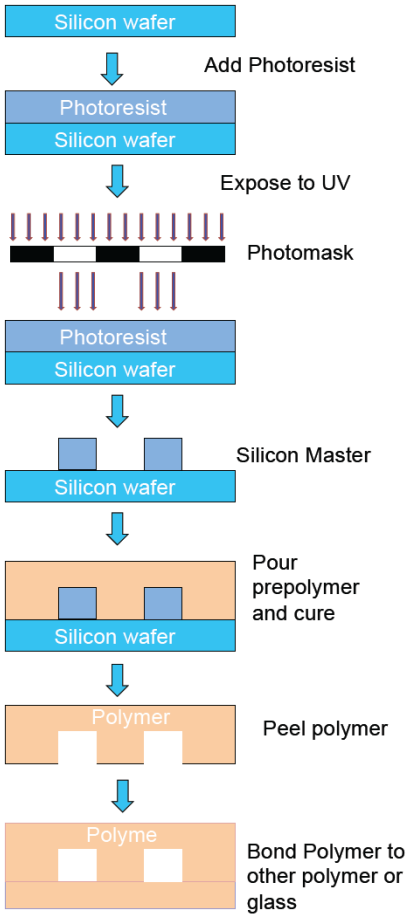

Fig. (2). Schematic of photolithography for polymer microdevice fabrication.

3. MICRORESERVOIR-BASED DRUG DELIVERY SYSTEMS

Microreservoir-based drug delivery has made possible the existence of the delivery system with smaller size and features to control drug delivery rates at different target sites in a more precise way. Drugs can even be delivered to target tissues or cells in a controlled manner that is usually unfeasible using traditional therapeutic methods. These reservoirs provide a well-controlled environment for drug formulation to increase drug stability and delivery times. Reservoir systems, which may be either external or implanted within the body, have the flexibility of the choice of delivery methods including pulsatile, on demand dosing and zero order [47]. These devices typically consist of reservoirs containing drugs, release control systems, and biodegradable polymer or metallic layers as the membrane. Therapeutic drugs which are sealed in a reservoir by metallic or polymer layers can be triggered to open or degrade when desired to release the drug by different approaches including pH, magnetic field, electric field, and temperature [22, 48, 49].

3.1. Silicon-based Microdevice

Microreservoir-based devices made up of silicon have been developed over years [50]. Macro- and nano-porous silicon has been widely used in drug delivery applications

[51]. Silicon-based reservoirs can achieve drug release by different triggers including electrochemical dissolution, magnetic force, telemetry, electronic force, and temperature. They typically have an array of cavity shape; with metallic lateral surface wall, the top and bottom of which is usually sealed by either a polymeric or metallic layers. Once the sealed layer is triggered to open, the loaded drug can be released from the microreservoir.

Loading of drugs into a microreservoir may degrade the drug due to harmful solvents or high temperatures. Initiated chemical vapor deposition (iCVD) coating does not expose the drug to harmful solvents and high temperatures, and it is independent of the surface chemistry and pore size of the nanoporous matrix. McInnes *et al.* did a proof of concept development of a pH controlled drug delivery system fabricated by functionalizing biodegradable porous silicon (pSi) by iCVD, with no drug degradation after loading into the pSi matrix [54]. Model drug camptothecin (CPT) was loaded into pores and capped with a thin film of pH responsive copolymer, poly(methacrylic acid-co-ethylene dimethacrylate) (p(MAAco-EDMA)) through iCVD. CPT release from uncoated pSi was the same in two buffers of pH 1.8 and 7.4, while drug release from pSi matrix coated with p(MAA-coEDMA) was 13.1 nmol/(cm^2 h) at pH 7.4 and 3.0 nmol/(cm^2 h) at pH 1.8, respectively. There was a significantly higher quantity of the drug release in a controllable rate at pH 7.4 (13.1% of the original payload over 10 h) than that at pH 1.8 (3.0% of the original payload over the same time frame).

MEMS manufacturing technologies have been widely used for the fabrication of different components of silicon-based drug delivery systems. Elman *et al.* developed an electro-thermally induced structural failure actuator (ETISFA) as an activation mechanism for implantable controlled drug delivery using MEMS [55]. The device consists of a reservoir (drugs stored in liquid or solid form), a sealing layer of silicon nitride (insulating the drug from the exterior and contains active portion of device), and a base port layer (orifice to fill the device). They performed the *in vitro* release experiments based on Joule heating to show repeatable release curves of mannitol-C^{14}. The drug release showed a first order release kinetics. The device provides a method to vary the flux and release rate on demand due to the ability to control the burst area of the membrane. Gensler *et al.* developed an implantable MEMS micropump system for the delivery of drugs in small animals with controlled timing and location of dosing [56]. The refillable device with inert drug reservoirs had an integrated electrolysis micropump. The fully integrated system under applied constant current of 1.0 mA and a power consumption of only ~3 mW, generated a flow rate of 4.72±0.35 μL/min. They showed the ability to deliver drugs to small animals with control over delivery rates and volume, with a preliminary success in using gene therapy in combination with radiation to combat cancerous tumors. Jeon *et al.* fabricated electrically responsive nanoporous membrane based on polypyrrole doped with dodecylbenzenesulfonate anion (PPy/DBS) that was electropolymerized on the upper surface of anodized aluminium oxide (AAO) membrane [11]. The pore size was actuated electrically (Fig. **3**). They confirmed the actuation by *in situ* flux measurement and atomic force microscopy. They demonstrated pulsatile (or on-demand) drug release by using fluorescently labeled protein as a model drug. In addition, Masi *et al.* developed MEMS-based microreservoir for temozolomide (TMZ) delivery in a 9L rat gliosarcoma model [52]. They confirmed the safety of implanting the device intracranially with preliminary *in vivo* studies. The silicon-based microreservoir had the inner dimensions such that it would contain a 10 mg payload of TMZ when loaded in a powder form and could be

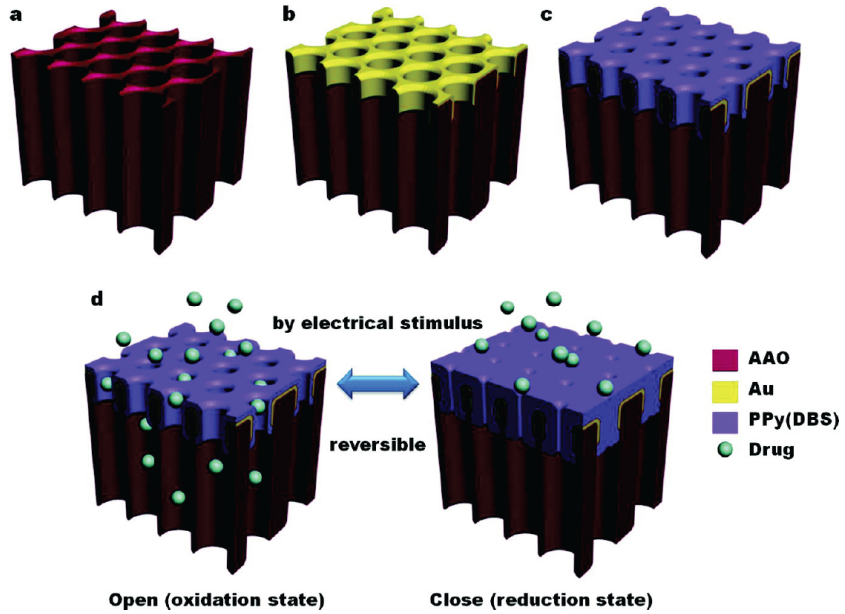

Fig. (3). Schematic to fabricate an electrically responsive microreservoir. (**a**) Fabrication of AAO membrane. (**b**) A thin gold layer on top and side wall of the membrane. (**c**) Polypyrrole electropolymerized on gold layer, and electrically responsive nanoporous membrane was fabricated at the oxidation state. (**d**) Reversible change of pore size (and drug release rate) between oxidation and reduction states. Copyright© with permission from 2011 American Chemical Society [11].

capped by a 3-membrane chip. The overall reservoir dimensions were 3.7 × 3.2 × 2.2 mm. Briefly, one side of the wafer was 720 × 720 μm regions of bare silicon. Titanium (30 nm) and gold (250 nm) layers were sputtered onto the same side of the wafer as the nitride membranes. Thin (40 mm) metallic 'fuses' were then defined using standard photolithography. TMZ delivered from the device was effective at prolonging animal survival.

A few reports of microreservoir-based drug delivery systems have been used for in-human testing. Farra *et al.* discussed the first in-human testing of a wirelessly controlled and implantable microchip-based drug delivery system [57]. Human parathyroid hormone fragment [hPTH(1–34)] was delivered from the device *in vivo* for the treatment of osteoporosis. The 13.0 mm × 5.4 mm × 0.5 mm silicon chip having 10 individually addressable, 600-nL reservoirs, containing discrete doses of lyophilized hPTH(1–34), were implanted in eight osteoporotic postmenopausal women for 4 months. The device was wirelessly programmed to release doses once daily for up to 20 days, which increased bone formation and produced similar pharmacokinetics to multiple injections but with lower coefficients of variation. The pharmacokinetics, safety, tolerability, and bioequivalence assessment showed no toxic or adverse events from the device, and patients stated that the implant did not affect quality of life.

3.2. Polymer-based Device

Polymer-based devices have been widely used in targeted and controlled drug delivery, due to the ease of fabrication and biocompatibility. Low-cost polymers have been successfully fabricated for administration in biopharmaceuticals as they are biocompatible, biodegradable and easily obtained naturally or be synthesized artificially. Biodegradable polymer-based microreservoirs are preferred to silicon-based microreservoirs for drug delivery as they can completely biodegrade and release the drug at a controlled rate at the desired site. In addition, there is no requirement of surgical removal of empty microreservoir device after the release of the drug. The diffusion coefficient of the drug can be altered according to needs by altering the size of drug molecules, the pore size or spacing between the polymer chain, and the composition of different polymers. Initiation of the release of the desired drug from multi-microreservoirs with different drugs can also be programmed into the device by controlling the composition and thickness of each membrane cap in the multi microreservoir system.

Polymer-based devices can be fabricated in a 3D format for drug delivery. Petersen *et al.* reported hot punching as a modified hot embossing method of fabricating high aspect ratio 3D polymeric microstructures forming a reservoir with a volume in the nanoliter range for drug delivery [58]. An elastic PDMS layer was deposited between the poly-L-lactic acid (PLLA) layer and the hard Si substrate. The 3D microcontainers had a diameter of 300 μm and depth of 90 μm resulting in a volume of approximately 4 nL per container. The fabrication process can be applied to other drug delivery devices or other application like tissue engineering where fabrication of individual 3D microstructures in polymer is required.

The development of stimuli-responsive controlled release system plays a pivotal role for the targeted drug delivery system to specific cells or tissues. Drugs loaded onto a polymeric microreservoirs can be triggered to release through different external stimuli including light and magnets. Timko *et al.* developed an implantable reservoir that was capped by a nanocomposite membrane whose permeability could be regulated by irradiation with a near infrared laser [59]. The reservoir displayed sustained and reproducible drug release for at least 3 h and short pulses over at least 10 cycles with an on/off ratio of 30 (Fig. **4**). The device that was loaded with aspart (insulin analog) achieved glycemic control after implantation in diabetic rats over a 2-wk period with reproducible dosing. Dosing was controlled by the intensity and timing of irradiation with negligible leakage between doses. *In vivo* studies were performed by implanting diabetic rats. The blood glucose concentration decreased after each dose, with minimum concentration occurring 150 min after the start of laser pulse (Fig. **4**). Similarly, Zaman *et al.* fabricated micro-patterned drug delivery device for light-activated drug release [60]. An ultraviolet cured biocompatible polyurethane device with 3 × 6 × 1.5 mm^3 dimensions were fabricated with 82 μm thick cap made from 3% poly-1,1-dichloroethylene. The device containing 10 % sodium fluorescein dye was implanted in the rabbit's eye with the cap facing towards the exterior of the eye. A suture, 6-0 prolene, was used to hold down the eyeball to create space for the implant. The device was implanted horizontally with respect to the cornea and placed between the sclera and sub-tenons space of rabbit's eye that was 0.5 mm away from the corneal limbus. After animal recovered from implant surgery, anhydrous glycerol was topically applied and the dye was released from the reservoir by a needle or an ophthalmic Q-switched Nd:YAG laser with the ablation threshold between 6 and 10 mJ to create 100-500 μm holes. The device elicited minimal inflammatory response and could be used for controlled release of drugs for certain ocular diseases. Pirmoradi *et al.* developed a magnetically controlled PDMS-based MEMS device for controlled release of an anti-proliferative drug, DTX, for the treatment of diabetic retinopathy for 35 days [53]. The drug-loaded microreservoir (Ø6 mm × ~550 μm), was sealed by an elastic magnetic PDMS membrane (Ø6 mm × 40 μm), which deforms and releases drug once the device is actuated in an external magnetic field. This proof-of-concept device controlled DTX release at a rate of 171 ± 16.7 ng per actuation interval for 35 days using 255-mT magnetic field. They tested the biological activity of released drug using human umbilical vein endothelial cells (HUVEC) and prostate cancer (PC3) cells and found that anti-proliferative effect of DTX was maintained over two months.

Microreservoir-based devices can have one or more reservoirs for the storage of drug formulation based on the required therapeutics. Tobias *et al*. developed reservoir-based, bioresorbable and elastomeric device for the controlled release of ciprofloxacin-HCL (CIP) [61]. They performed an *in vitro* evaluation of the implantable device made of poly(glycerol-co-sebacic acid) (PGS) casted in a tubular geometry with solid drug powder packed into its core and a short term release through osmosis and diffusion mechanisms from the orifice drilled through its wall. The *in vitro* testing showed the device was stable to function as a semi

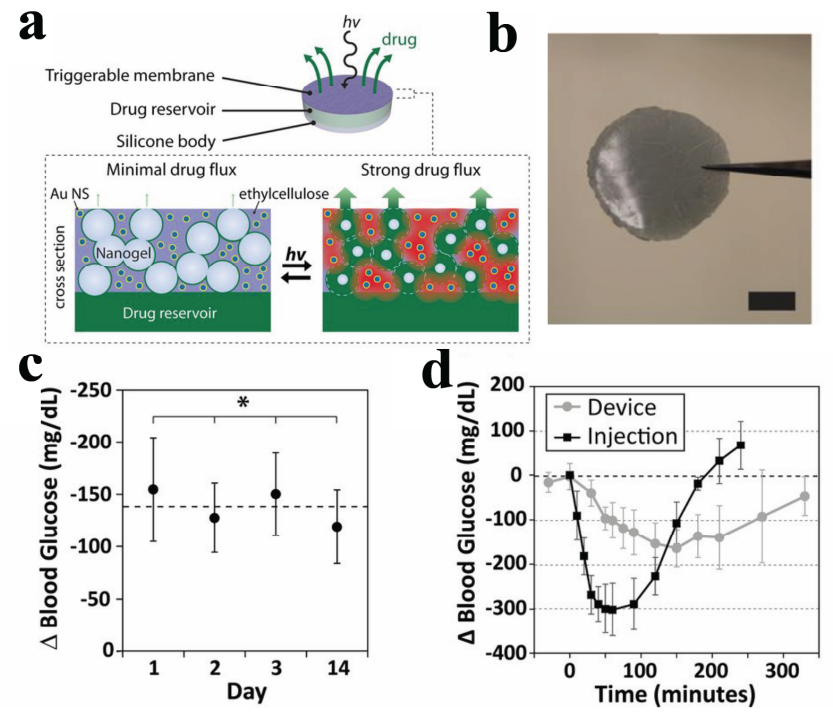

Fig. (4). Polymer-based microreservoir. (**a**) Schematic of proposed deveice (upper) and membrane cross-section (lower); (**b**) Photograph of a nanocomposite membrane (scale bar: 1 cm); (**c**) The average depression of blood glucose after device implantation at 150 min is shown with a dotted line; (**d**) Comparison of blood glucose response after administering 1U aspart by subcutaneous injection or by triggered release from devices. Copyright© with permission from 2013 PNAS [59].

permeable material and orifices with 100-150 μm were found to allow zero-order release kinetics. Approximately 4 μg/ml of CIP per hour could be released into the 3-4 ml fluid capacity of the seminal vesicle and would be capable of killing most species of gram negative bacteria responsible for chronic prostatitis (CP). Sometime it is desired to release multiple drugs at different dosage at a desired rate based on the property of the polymer. Chirra *et al*. developed a poly(methyl methacrylate) (PMMA) based multiple reservoir bioadhesive microdevice using photolithography and reactive ion etching for independent rate controlled multiple drug delivery [62]. They entrapped three different model drugs through photo-polymerization within separate reservoirs to provide simultaneous release solely dependent upon the property of the respective encompassing polymer/hydrogel matrix. It was used to deliver multiple drugs at different rates in localized regions. They also observed enhanced bioadhesion of the microdevices in the presence of a conjugated targeting protein (tomato lectin) to the PMMA surface. The device may be effective for administration of a broad range of therapeutics to orally deliver and treat intestinal diseases including inflammatory bowel disease (IBD) and irritable bowel syndrome (IBS) or for co-delivery of permeation enhancers.

4. MICRONEEDLE-BASED DRUG DELIVERY SYSTEMS

Transdermal drug delivery is an alternative to conventional drug delivery methods including oral administration and injection, but many therapeutic drugs are limited to reach systemic circulation due to the presence of biological barrier of the skin like stratum corneum (SC). Transdermal delivery of hydrophilic drugs and macromolecules (molecular weight > 500 Da) may not be successfully administered transdermally. Reversible disruption or by-pass of SC molecular architecture may be required for the drug to penetrate the SC. Microneedles (MNs) that can puncture skin, and bypass the SC to form transient aqueous transport pathways, were developed to increase the permeability of the drug. These MNs puncture the skin for the delivery of hydrophilic drugs and macromolecules, including peptides, DNA and other molecules, which cannot penetrate the SC of the skin [43]. MNs penetrate the skin through the SC and into the viable epidermis (VE) so that they avoid contact with the dermal layer with nerve fibers and blood vessels [63]. MNs consist of several micro-projections of different shapes attached to a base support and generally 25-2000 μm in height. In addition, MNs have reduced needle insertion pain and tissue trauma. They have been widely used as devices for pain-free intradermal delivery of bio-macromolecules [64].

Figure **5** shows the schematic of different types of MNs. Solid MNs can be applied and then removed to create micropores in the skin. Transdermal patches can be applied over the micropores in the skin so that the drugs are released to the targeted site through the micropores. Coated MNs are the MNs coated with drug molecules and they can be applied directly to the desired area for the instant delivery of the drug after which they can be removed. Polymeric MNs remain in skin and dissolve over time to deliver the drug within the targeted site at the rate pre-determined by the dissolution rate

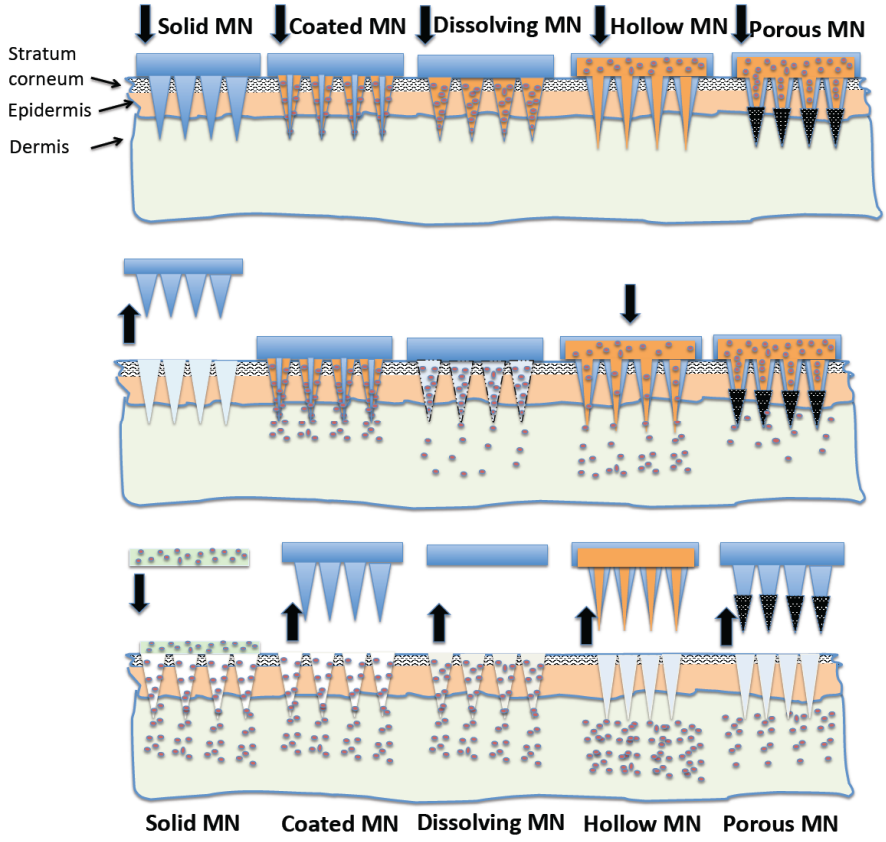

Fig. (5). Schematic of different methods of MNs application across the skin.

of the MN. Hollow MNs can be used for continuous drug delivery or body fluid sampling. Drug solutions stored at the top reservoir are released from the hollow MNs at the desired site by the application of pressure. Porous MNs, which differ from hollow MNs by the presence of the porous tips, have the solid or liquid formulation of the drug within the MNs. Drug diffuses to the targeted site when hydrated with the interstitial fluid. Table **1** summarizes the applications and delivery routes of different MN-based drug delivery systems.

MNs ought to be inserted into the skin in a controlled and reproducible manner for a successful reproducible delivery of the drug. The application of MNs requires the aid of applicator devices to present the MN array to the biological target or have to be manually applied, which is unlike the conventional patch-based delivery system. Applicator devices provide uniform pressure and penetration, which is difficult to achieve by manual application [65]. Recently, the penetration ability of low-density arrays (42 MNs/cm^2) with 750-µm long MNs, applied manually or by using a snap-based applicator, was investigated with no serious adverse events associated with the use of patches [66]. Similarly, Coleman *et al*. compared two groups receiving either self-administration or healthcare-provider-administration of influenza vaccine using a hollow microneedle (HMN) device to see the immunogenicity, reactogenicity, success rate, and acceptability of self- versus nurse-administered intradermal trivalent seasonal influenza vaccine [67]. Self-administered vaccine was immunologically non-inferior and reached all European medicines agency (EMA) immunogenicity criteria as compared to nurse-administered intradermal influenza vaccine. These kinds of study suggest that it may be feasible for adult people to self-administer intradermal influenza vaccine using the devices. In addition, self-administered vaccine may also reduce the cost of vaccination. Simple administration with MN patches may enable vaccination by patients themselves in rural settings or by minimally trained workers. More researches need to be done to improve the reliability of MN patches administration, reproducibility, and acceptability. In addition more clinical trials on the immunogenicity of vaccine, efficiency of the drug, and safety of self-administration should be conducted.

4.1. Solid Microneedles (SMNs)

In SMNs-based drug delivery systems, SMNs are pressed against the skin's surface to physically disrupt the SC to create micron sized transient pores through which drug can be transported, either for local effect in the skin or for systemic delivery after uptake by skin capillaries. Therapeutic drugs can then be applied over the surface by drug-loaded patches or using semi-solid topical formulation including gel, lotion, cream or ointment. It has been shown that SMNs can increase permeability even four orders of magnitude *in vitro* for molecules up to 100 nm in diameter. The mechanical strength of SMNs can be varied by the choice of MN material and geometry while the force needed to insert MNs into tissue can be controlled by the tip sharpness. SMNs have been fabricated from different materials including silicon, photolithographic epoxy, co-polymer of methylvinyl ether

Table 1. Summary of different microneedle systems for controlled drug delivery.

Drug delivery device	Application	Delivery route	Drug	Fabrication material	Ref.
SMNs	Insulin therapy	GI tract	Insulin	Acrylic	[71]
	Anti-Hypertension	Transcutaneous	Verapamil & Amlodipine	Stainless steel	[72]
	Immunization	Transcutaneous	Ovalbumin Antigen	-	[73]
	Delivery of therapeutic peptides	Transdermal	Peptides	-	[74]
	Multiple drug delivery	Transdermal	Insulin	Silicon	[75]
Coated MNs	Vaccination	Intraepidermal	Asparginase	-	[77]
	Genetic skin disease & immunization	Skin	Plasmid DNA	Stainless steel	[78]
	Cancer treatment	Intratumoral	DOX	Stainless steel	[79]
	Neovascularization	Intracorneal	Bevacizumab	-	[80]
	Analgesic	Skin	Lidocaine/Prilocaine	Polymer	[81]
	Vaccination	Skin	Influenza vaccine	Titanium	[82]
	Vaccination	Skin	Influenza (H1N1) vaccine	-	[83]
	Vaccination	Lip & tongue	HIV Antigen	Stainless steel	[84]
HMNs	Fecal incontinence	Perianal skin	Phenylephrine	-	[85]
	Eye treatment	Sclera	Sulforhodamine B	Borosilicate	[86]
	Treatment for diabetes	Subcutaneous	Lispro insulin	-	[88]
	Polio vaccination	Intradermal	Polio vaccine	Silica	[89]
Porous MNs	Vaccination	Skin	DC-SIGN	Ceramic	[91]
	Insulin therapy	Skin	Insulin	Titanium	[92]
	Analgesic	Skin	Lidocaine	Poly(ethylene glycol) diacrylate	[93]
Dissolvable MNs	Insulin therapy	Transdermal	Insulin	PMVE/MAH	[98]
	Growth hormone	Skin	hGH	Carboxymethyl cellulose & trehalose	[96]
	Influenza vaccination	Skin	Influenza virus	PVP	[100]
	Vaccination	Transcutaneous	Ovalbumin Antigen	PVP	[101]

and maleic anhydride (PMVE/MA), polycarbonate, PMMA, PLGA, polyglycolic acid (PGA), polylactic acid (PLA), and metals like titanium, tantalum, nickel and ceramics [43, 68, 69]. Before using MNs for clinical practice it is essential to understand how the skin penetration is effected by different factors such as force applied and the diameter of these MNs. Römgens *et al*. monitored the penetration process of individual MNs with varying tip diameters [70]. Single MNs were inserted in human *ex vivo* skin and the surface of the skin was monitored while measuring the force of MN. The average penetration depth at 1.5 mm displacement was similar for all tip diameters and MNs with a tip diameter of 5 μm were smoothly inserted into the skin, while the penetration depth of MNs with a larger tip diameter suddenly increased after initial superficial penetration. Force at insertion linearly increased with tip diameters ranging from 20 to 167 mN. It shows that sharp MNs are essential to insert MNs in a well-controlled way to a desired depth.

Although oral administration of drugs is the most convenient route, it is not preferred because of the hostile environment of the gastrointestinal (GI) tract. Traverso *et al*. presented a proof-of-concept use of MNs for the delivery of biologics via the GI tract [71]. The device fabricated from clear acrylic had 25G needles protruding 5 mm from the surface and were fitted into the orifice. The device, 2cm in length and 1 cm in diameter, was endoscopically administered in the stomach of the Yorkshire pigs. Both the hollow and solid MNs device gets revealed in the desired location in the GI tract when the coating of the device dissolves. In HMNs, the drug reservoir is compressed through peristalsis to release a drug, while in coated SMNs, the MNs penetrate tissue and break off of the pill leaving the needle to release

drug in controlled manner depending upon the drug formulation. The blood glucose response kinetics of insulin was significantly improved compared to the subcutaneous route. They also showed that device with radially exposed protruding MNs could safely pass via the GI tract without any evidence of tissue damage.

The efficiency of drug delivery can be improved by several methods including the use of rollers and patches. Kaur *et al*. studied the effect of stainless steel SMNs and MN rollers on percutaneous penetration of verapamil hydrochloride and amlodipine besylate [72]. 2-(3,4-dimethooxyphenyl)-5-[2-(3,4 dimethoxyphenyl)ethyl-methyl-amino]-2-propan-2-yl-pentanenitrile commonly called as Verapamil and (R, S)-2-[(2-aminoethoxy) methyl]-4-(2-chlorophenyl)-3-ethoxycarbonyl-5-methoxycarbonyl-6-methyl-1, 4-dihydropyridine called as Amlodipine are calcium channel blockers and their passive penetration across the skin is low. They used scanning electron microscopy to view stainless steel MNs and microconduits. The created microconduits determined the disruption of SC, a barrier to transdermal penetration, showing successful penetration of skin to create micropores. Passive diffusion through untreated porcine skin was taken as control. Transcutaneous flux of verapamil increased from 8.75 μg/cm^2/h to 49.96 μg/cm^2/h in the MN-roller treated porcine skin, while percutaneous flux of amlodipine besylate increased from 1.57 μg/cm^2/h to 22.39 μg/cm^2/h after the use of stainless steel MNs. These studies could lead to development of transdermal MN patches for these antihypertensive drugs. Conjugation of drugs with NPs or biocapsules can also increase the efficiency of drug delivery. Kumar *et al*. studied the permeation of antigen protein-conjugated NPs (230 nm) and live bacteria through MN treated mouse skin [73]. They found that SMNs with ovalbumin conjugated on their surface could permeate through mouse skin pretreated with MNs. In addition, transcutaneous immunization induced a stronger antiovalbumin antibody response than using ovalbumin alone. They also found that transcutaneous immunization on a MN treated skin could potentially induce a stronger immune response. The risk of bacterial infection associated with microneedle treatment was similar to hypodermic injection, as the skin permeation of live *Escherichia coli* was not greater than that enabled by hypodermic injection.

Microneedle arrays have been used widely for the delivery of drugs as they can enhance the delivery of the desired drugs. Zhang *et al*. studied the use of solid microneedle arrays (SMNA) (150 μm in length) in transdermal peptide delivery and examined the relationship between peptide permeation rates and D_2O flux [74]. The influence of MN pretreatment on skin permeation was evaluated using porcine ear skin with Franze diffusion cell. It was found that peptide permeation increases significantly after MN pretreatment and its rate was inversely related to the molecular weight of peptide (Permeation rate of peptides decreases with the increase in molecular weight). Convective solvent flow may contribute to the enhanced transdermal peptide delivery because positive correlation was found between D_2O flux and acetyl hexapeptide-3 clearance. The study shows that SMNAs are effective devices to enhance skin delivery of peptides and to provide a sustained release during 24 h. Vinayakumar *et al*. fabricated an array of rectangular cup shaped silicon MN with a height of 200 μm and length and breadth of 60 μm each [75]. The cups were filled with drug using an in-house built drop coating system. It was possible to fill the cups selectively with different drugs for simultaneous multiple drug delivery. Successful drug dissolution was observed when the coated MN was used on female nude mice (Nude HSD-Fox N1) of 6–8 weeks age, weighing between 18 and 22 g. Maaden *et al*. fabricated a pH sensitive MNA with inactivated polio vaccine (IPV) and N-trimethyl chitosan chloride (TMC)[76]. The immunogenicity was assessed after the topical application of the coated MNs in rats. The 200 μm long MNs were alternately coated with 10 layers of IPV and TMC (Fig. **6**). IPV specific antibody was induced, illustrating that they were practically applicable.

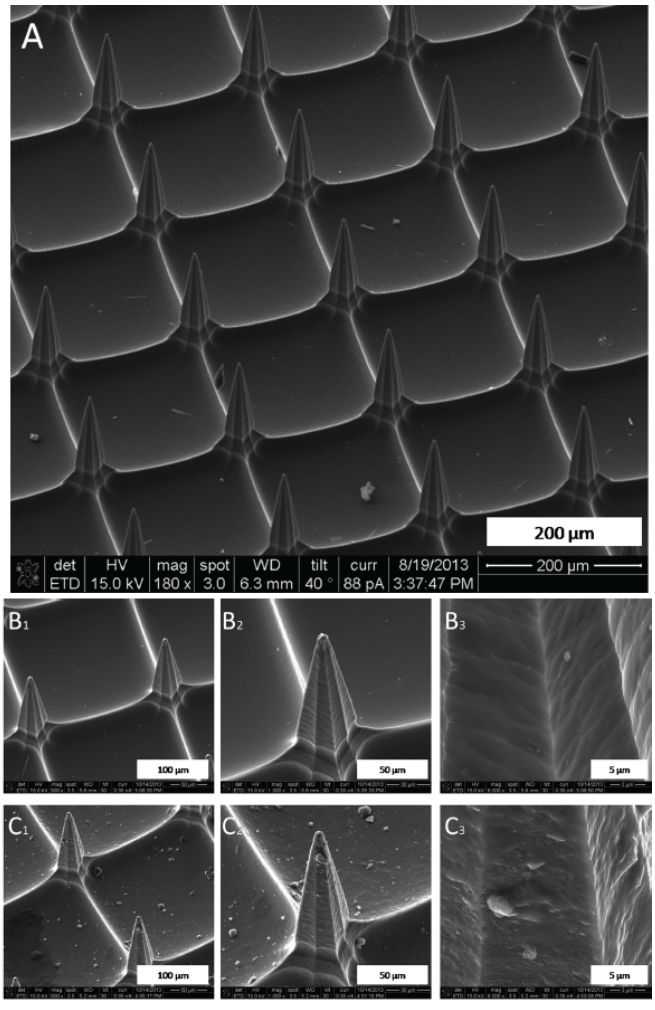

Fig. (6). SEM images of MNs. (**A** and **B**) Nanomodified MNs and (**C**) MNA coated with 10 layers of IPV alternated with TMC at a magnification of 500 (1) 1000 (2) and 8000 times (3). Copyright© with permission from 2015, American Chemical Society [76].

4.2. Coated Microneedles

MNs coated and dried with therapeutic drugs on the surface may enhance the long-term stability of the drugs, which is a rapid method for drug delivery, especially for vaccine delivery to the skin. MNs can be coated with a drug in a formulation suitable for coating and subsequent dissolution

so that the drug can be delivered as soon as the MNs are inserted into the tissue. Coated MNs are limited by the amount of drugs that can be coated onto the tip and shaft of the MNs. The summary in Table **1** shows that the coated MNs have been mostly used for vaccination.

Coated MNs can be used for the delivery of different therapeutics including protein, DNA, and anticancer drugs. Witting *et al.* did the feasibility study for intra-epidermal delivery of protein using SMNA with needle length of 300 μm [77]. MNs were coated with protein concentration between 10 and 23 μg. They reported 90% of the bioactivity of the model protein asparaginase for 3 months. Skin experiments showed 68.0 ± 11.7% of intraepidermal deposition of the coated model protein after single application with minor skin irritations. Following intradermal application, the coating formulation dissolved rapidly resulting in homogeneously distributed protein in the epidermal layer. Pearton *et al.* excised human skin explants to investigate and optimize the parameters for stable and effective MN facilitated pDNA delivery [78]. They optimized a dip-coating method to increase the loading capacity up to 100 μg of pDNA per 5-MNA. They were able to reproducibly perforate human skin at low (< 1 N) insertion forces using coated MNs. Addition of saccharide excipients increased the physical activity without decreasing the biological functionality of pDNA. They reported the gene expression of the reporter gene in viable human skin by the use of pDNA-coated MNs. This kind of MN delivery of nucleic acids to the skin can represent a new potential approach for the clinical management of genetic skin diseases and cutaneous cancers, along with intracutaneous genetic immunization. Ma *et al.* developed coated MNs as a direct and minimally invasive intratumoral delivery of anti-cancer drugs [79]. Microscopic evaluation of 3D tissue phantoms and porcine cadaver buccal tissues that were treated with inplane (1D) MNs coated with DOX encapsulated PLGA NPs demonstrated that DOX could diffuse both laterally and vertically into tissues and produce cellular cytotoxicity. Similarly, out of plane (2D) MNAs measuring 1 cm x 1 cm with 57 MNs coated with free DOX could produce uniform distribution of DOX in a porcine cadaver buccal tissue up to a depth greater than 3 mm. Hypodermic injection into a porcine buccal tissue however, confirmed significant leakage of the injected volume (about 25% of the injected 80 μL) in addition to causing pain to patients and poor distribution of the drug in the tumor.

Coated MNs have also been used for the treatment of injury either for the delivery of analgesic agents or for neovascularization. Kim *et al.* used SMNs for the intracorneal delivery of bevacizumab to treat injury induced neovascularization [80]. SMNs, 400 μm in length were coated with bevacizumab using a rapidly dissolving formulation. Corneal neovascularization was first induced in the eye of New Zealand white rabbits by a 7-gauge silk suture that was placed 1mm from the limbus. The MN delivery (a single bolus of approximately 1.1 μg of bevacizumab) was compared against topical eye drop (bevacizumab, 25 mg/mL, given three times per day for 14 consecutive days) and subconjunctival injection (100 μL of bevacizumab, 25 mg/mL). Digital photographs were taken, and the area of neovascularization was also measured for 18 days. It was found that the MN approach was more effective in suppressing neovascularization after suture-induced injury using much lower dose as compared to other conventional methods. It shows that MNs could be used to deliver protein therapeutics locally and with minimal invasion into the intrastromal space of the cornea. Zhang *et al.* developed Lidocaine-coated MN for rapid, safe and prolonged analgesic action [81]. They fabricated polymeric MNs dip-coated with aqueous lidocaine formulation, the amount of which was determined by high performance liquid chromatography (HPLC) and then inserted into domestic swine. They used commercial lidocaine/prilocaine Eutectic Mixture of Local Anesthetic (EMLA) cream as a control. Skin punch biopsies were then collected and lidocaine concentration in skin was analyzed by HPLC-mass spectroscopy (LC-MS) to access drug delivery and pharmacokinetics. They found that lidocaine dissolved into the skin in ~1 min and exceeded the lidocaine level needed to cause analgesia (100 ng/mg). Co-formulation with 0.03 wt% vasoconstrictor-epinephrine maintained the concentration of lidocaine in the tissue above 100 ng/mg for approximately 90 min. It showed that these coated MNs could be used to deliver drugs to the skin within minutes. MNs provide rapid onset of local analgesia and facilitate routine or emergency procedures.

MN patches for vaccine delivery have received increasing attention, as it is a simple, reliable, and low-cost approach. It can be self-administered, and patches can be removed after a while. They even show stronger immune response than IM vaccinations. Most of these studies were done using freshly prepared MNs, so the long-term stability of the vaccine coated onto MNs needs to be studied further. Choi *et al.* studied the long term stability of the whole inactivated influenza vaccine coated onto MNs [82]. Their *in-vitro* studies showed that vaccine lost its stability as measured by hemagglutination activity in proportion to the degree of coating matrix crystallization and phase separation. They observed damaged morphology of the inactivated virus vaccine as seen through transmission electron microscopy (TEM). Reduced vaccine immunogenicity was also observed after influenza vaccination using MNs with crystallized or phase-separated coatings in the *in vivo* studies. Inhibition of the phase changes in the vaccine coating film is needed for the long-term stability of the vaccine-coated MNs because crystallization and phase separation of the vaccine coating damages the vaccine and can render it completely non-immunogenic. As the vaccines delivered by coated MNs are effective, it is desired to study the effects of adjuvants using this approach. Weldon *et al.* studied the effect of adjuvants (TLR ligands; Toll-like receptors such as lipopolysaccharide, poly(I:C) and imiquimod) on response to skin immunization by MNs coated with Influenza subunit vaccine [83]. BALB/c mice were given 1 μg of monovalent H1N1 subunit vaccine alone or with 1 μg of imiquimod or poly(I:C) individually or in combination through coated MN patches inserted into the skin. Although, poly(I:C) adjuvanted subunit influenza vaccine induced similar antigen-specific immune responses, imiquimod-adjuvanted vaccine elicited higher levels of serum IgG2a antibodies and increased hemagglutination inhibition titers compared to vaccine alone. In addition, it induced a robust IFN-γ cellular response compared to vaccine alone. It supports the use of TLR7 ligands as adjuvants for skin based influenza vaccines. Similarly, Ma *et al.* studied the feasibility of the use of coated MNs to deliver vaccines

into the oral cavity so as to induce systemic and mucosal immune responses [84]. MNs were first coated with sulforhodamine, ovalbumin and two HIV antigens and then inserted into the inner lower lip and dorsal surface of the tongue of rabbits. The penetration of MNs into the lip and tongue of rabbit was confirmed by histological evaluations. It was found that the lip and the tongue are equally immunogenic sites for vaccination by using ovalbumin as a model antigen as both sites induced a significant secretory IgA in saliva as compared to pre-immune saliva. Two HIV antigens, a virus-like particle (E2V3) and a DNA vaccine (gp160 HIV DNA) were used to compare MN-based oral cavity vaccination to the intramuscular route. They expressed similar levels of antigen-specific immunoglobulin G (IgG) in serum, and only MN-based oral cavity vaccination group stimulated a significantly higher antigen-specific Immunoglobulin A (IgA) response in saliva, but not intramuscular injection. It was found that the coated MN delivery of vaccines to the oral cavity could activate both systemic and mucosal immunity, and the intramuscular method could only activate systemic immunity.

4.3. Hollow Microneedles (HMNs)

HMNs consist of MNs with fine perforates. These MNs have drug solutions, which can be delivered continuously and don't require the replacement of MNs with drug patches as in case of SMNs-based drug delivery systems. They provide a defined duct for pressure driven flow of the formulations of therapeutic drugs into the skin or tissue at a desired flow rate. HMNs can also be used as a conduit for drug delivery into the tissue from a non-pressurized drug reservoir. Jun *et al*. used 1.5 mm HMNs for targeted delivery of phenylephrine for the treatment of fecal incontinence into the anal sphincter muscle through the perianal skin to increase the resting anal sphincter pressure [85]. Compared to intravenous (IV) injection, subcutaneous (SC) injection and intramuscular (IM) injection treatments, HMN treatment produced greater anal pressure with the maximum anal pressure between 5 and 6 h with no increase in blood pressure in female Sprague–Dawley rats. 12-hour increase in the resting sphincter muscle pressure showed the possibility of treatment of fecal incontinence. This new treatment could be of great potential because of the ease of use, minimal pain and dose-dependent response.

HMNs have been successfully used to deliver drugs to different parts of the body including eyes and skin. There are several reports of *ex-vivo* delivery of drugs to the eye of humans and other animals. Patel *et al.* inserted a single HMN into the sclera and infused sulforhodamine B, NPs and microparticles suspensions into the suprachoroidal space to target the posterior segment of the eye in a simple and minimally invasive way [86]. They used whole rabbit, pig, and human eyes *ex-vivo* for the experiments. Successful particle delivery was imaged using bright field and fluorescence microscopy as well as microcomputed tomography. Needle lengths of 800–1,000 μm and applied pressures of 250–300 kPa was found to be most reliable to deliver volumes up to 35 μL consistently. This experiment shows that MNs may provide a minimally invasive method for controlled drug delivery to the back of the eye. Lyon *et al*. fabricated carbon nanotube-polyimide composite HMNs for transdermal delivery of a drug [87]. Pattern bundle of carbon nanotube was first used as a porous scaffold after which polyimide resin was wicked through for the structure and support to penetrate the skin. Simple and scalable HMNs could be created in a single step owing to high aspect ratio and bottom-up assembly of carbon nanotubes. They successfully demonstrated the delivery of aqueous methylene blue dye into hydrogel and swine skin *in vitro*. MNs did not sustain any structural damage, which was confirmed by electron microscopy of MNs after delivery.

HMNs have also been widely used for the *in vivo* delivery of drugs either in the human bodies or the experimental model animals. Norman *et al.* showed that there is faster pharmacokinetics and increased patient acceptance of intradermal delivery of insulin using a single HMN in children and adolescents with type 1 diabetes (T1DM) [88]. 16 children and adolescents with T1DM were given Lispro insulin by a MN and subcutaneous administration. It was found that the MN insertion pain was significantly lower compared to subcutaneous catheter. In addition, the insulin onset and offset time was 22 min and 34 min faster respectively after the HMN delivery as compared to subcutaneous delivery. Maaden *et al.* studied the depth-controlled microinjection mediated dermal delivery of polio vaccine in rats using HMNs [89]. HMNs with an inner diameter of 20 μm produced by hydrofluoric acid etching of fused silica capillaries and electromagnetic applicator were used for the controlled delivery in *ex-vivo* human skin with controlled insertion speed (1-3 m/s), depth (0–1,000 μm), and angle (10°–90°) without clogging or breakage of the needles. Rats were then immunized with inactivated poliovirus vaccine (IPV) by an intradermal microinjection of 9 μL at a depth of 300 μm and an insertion speed of 1 m/s. Intradermal microinjection of IPV induced immune responses (IPV-specific IgG and virus-neutralizing antibodies) comparable to those elicited by conventional intramuscular immunization.

4.4. Porous Microneedles

Porous MN is a single unit drug delivery system with the whole porous MNA along with the backplate containing a liquid or dry formulation of a drug. In liquid formulation, drug diffuses from the MN matrix into the skin where it is pierced. MNs remain inside the skin and the drug diffuse from the drug reservoir via the MNs into the skin. For the dry formulation, dried drug is loaded into the pores of the MNs and when it pierces the skin the drug formulation is hydrated with the interstitial fluid (ISF), which can occur through the capillary force of the pores and the drug diffuses. Basically porous MNs-mediated drug delivery is a diffusion-based process [90].

Different fabrication procedures including micromolding, etching, and photolithography have been used to fabricate the porous MNs for different applications. Verhoeven *et al.* used ceramic nanoporous MNA as a transport interface in eggplants and an *ex-vivo* human skin model [91]. Micromolding process using a PDMS mold, generated through a double replication process from a SU-8/Si-master, was used as a template to prepare nanoporous MNA of Al_20_3. MNA in which porosity was related to the temperature used for sintering (80 nm between 1300-1500 ^{0}C) was shown to allow both the

delivery of substance and extraction of compounds using eggplants. *Ex vivo* human skin model was then used to deliver a labeled monoclonal against a specific marker, DC-SIGN (FITC labeled), which is representative for dendritic cells when activated by an antigen using a MNA. Post staining analysis revealed that intradermally targeted DCs were fully active. Yan *et al.* fabricated Ti MNs for drug delivery [92]. MNs were fabricated by the process of cutting and wet etching where each MN (height > 400 μm and pitch ~ 800 μm) consisted of connecting micro holes (20 μm in diameter) that delivered drug into organisms conveniently and efficiently. The MNs could resist large shear forces and pierce into the skin easily. They did the *in vivo* experiment into the rats by a patch of the MNs, which demonstrated that the MNs could deliver drugs into organisms to treat diseases without fracture. Kochhar *et al.* developed MN integrated transdermal patch (MITP) for fast onset and sustained delivery of Lidocaine [93]. Figure **7I** shows images of the fabricated MITP containing rhodamine B and various layers of MITP. MNs fabricated by photolithography-based process can create micrometer-sized channels in the skin to deliver lidocaine rapidly. The reservoir patch holding the bulk of the drug enabled higher drug loading and carried on to release the drug for prolonged periods so that drugs were diffused out of MNs through the porous channels. These MITP could encapsulate up to 70 mg of lidocaine. *In vitro* studies in rat skin showed that a significantly higher amount of lidocaine was delivered with a faster onset of drug permeation (within 5 min of application) by MITP as compared to commercial patches. As can be seen from Fig. **7II** a tightly packed polymer structure is observed and the increase in concentration makes the surface more rough and irregular which allows better interaction with the release medium, increasing the drug release. SEM images of MNs taken after the release of drug had smooth surface indicating most of the drug was released.

4.5. Dissolvable Microneedles

In dissolvable MNs-based drug delivery systems, the MN material dissolves or get biodegraded when it comes in contact with the interstitial fluid of the skin so that drug molecules are released from the matrix either for systemic or local delivery. These polymeric MNs in contrast to coated MNs are developed so that they can completely dissolve in the skin and leave no sharp biohazards waste after the treatment. They can be used as skin pretreatment to increase drug permeability or drugs can be encapsulated within MNs to release into the skin. Polymeric MNAs are gaining attention as minimally invasive transdermal drug delivery devices due to their effective localized drug delivery along with improved patient convenience and safety [94].

Polymer dissolvable MNA can be fabricated and/or replicated in a considerably more cost effective way as compared to a MNA made of silicon and metals [96]. Cha *et al*. developed a simple and cost effective method for fabrication of solid biodegradable polymer MNA for the transdermal drug delivery using acupuncture MNs [97]. A master template with acupuncture MNs, was prepared by fixing them onto a plastic substrate with selectively drilled holes, which determine the aspect ratio. MNA was fabricated from a biodegradable polymer, polylactic acid (PLA) by a micromolding process with a PDMS mold containing the cavity of the MNs, which was obtained by the PDMS replica molding

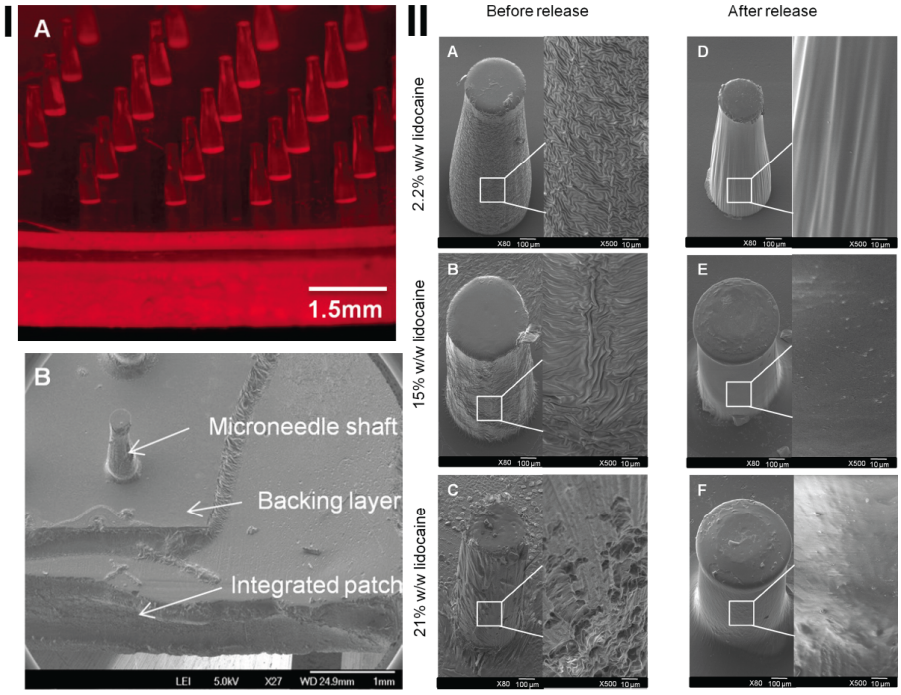

Fig. (7). Porous MNs. (I) Images of MN integrated transdermal patch (MITP) during fabrication. (**A**) MNs with encapsulated rhodamine B. (B) A scanning electron microscope (SEM) image of single porous MN. (II) SEM of MITP before and after release test. MNs containing (A) 2.2 %, (**B**) 15 %, and (**C**) 21 % (w/w) lidocaine before release and (D), (E), and (F) after release, respectively. Copyright© with permission from 2013 American Chemical Society [93].

against the master template. Pig cadaver was then used for two different methods of penetration and staining to examine the efficiency of transdermal drug delivery. Martin *et al.* fabricated biodegradable sugar glass MNs for transdermal drug delivery applications [95]. They created solid amorphous sugar glasses, which contained low residual quantities of water. It was created by dehydration of trehalose and sucrose sugar combination. The low temperature vacuum deposition micromoulding method was optimized to fabricate biodegradable sugar glass MNs that had sufficient structural rigidity to efficiently penetrate excised human breast skin. Sugar glass MNs with a marker compound dissolved rapidly and completely *in situ* to release a dye into deeper skin layers. These kinds of MNs can be used to deliver therapeutic drugs through the transdermal route.

The structure, height, and application pressure of the MNs directly impact the delivery of the therapeutic drugs. Garland *et al.* developed dissolvable polymeric MNA for electrically assisted transdermal drug delivery [98]. They studied the effect of MN height and MN density on the transdermal delivery of small hydrophilic compounds (theophylline, methylene blue, and fluorescein sodium) across neonatal porcine skin *in vitro*. They found that an increase in MN height and density led to an increase in the extent of transdermal drug delivery of peptide (bovine insulin) and protein (fluorescein isothiocyanate-labeled bovine serum albumin (FITC-BSA)) with highest transdermal drug delivery in MN design containing 361 MNs/cm^2 of 600 μm. It was found that the extent of peptide/protein release was significantly enhanced when iontophoresis (ITP) was used in combination with the soluble poly (methyl vinyl ether co maleic acid) (PMVE/MA) MNA for precise electric control of transdermal delivery. In addition, the secondary structure of model peptide insulin or model protein FITC-BSA was not adversely affected by incorporation of biomacromolecules into the PMVE/MA MNA. The application of electric current also enabled the permeation of macromolecules from the entire MNA matrix, and not just from the MN alone, thus increasing the efficiency.

Use of the polymeric dissolvable MN shows higher efficiency than the conventional injection. Lee *et al.* designed a dissolvable MN patch for simple and painless administration of biopharmaceuticals, human growth hormone (hGH) [96]. They encapsulated hGH within a 600 μm long dissolvable MNs composed of carboxymethylcellulose and trehalose. They observed complete hGH activity after storage at room temperature and humidity for up to 15 months. Pharmacokinetics of the hormone when the patch was manually inserted into the skin of hairless rats was similar to the conventional subcutaneous injection. After the patch was removed, MNs were almost completely dissolved, leaving behind blunt stubs and caused only slight transient erythema. Liu *et al.* delivered relatively high molecular weight drugs (fluorescein isothiocyanate-labeled dextran with an average molecular weight of 4 kDa (FD4)) using self-dissolving MNA that was fabricated from hyaluronic acid [99]. MNA significantly increased transepidermal water loss (TEWL) and reduced transcutaneous electrical resistance (TER), which indicated successful skin puncture to create drug permeation pathways. Histological analysis of the MNA showed uniform puncture of the skin and delivery of FD4 to the dermis and its rapid release after the dissolution of the MNs. Both TEWL and TER recovered rapidly as compared to tape stripping treatment, which showed that skin disruption caused by MNA was reversible. It was found that transdermal permeability of FD4 using the MNA was much higher than that of the FD4 solution and MNA increased the amount of FD4 accumulated in the skin more effectively.

Dissolvable MNs have also been used for vaccination or immunization. Sullivan *et al.* developed dissolvable polymer MN patches for influenza vaccination using a simple patch-based system that targets delivery to skin's antigen-presenting cells [100]. Inactivated influenza viruses were encapsulated in a biocompatible polymer for insertion into the skin and dissolution in the skin within minutes. Compared to intramuscular injection, MN vaccination generated robust antibody and cellular immune responses in mice that provided complete protection against lethal challenge as observed by more efficient lung virus clearance and enhanced cellular recall responses after the challenge. Guo *et al.* developed a transcutaneous immunization (TCI) device consisting of dissolvable polyvinylpyrrolidone (PVP) MNA in which the tips were loaded with antigen and adjuvant encapsulated in liposomes [101]. For co-delivery of antigens and adjuvants, ovalbumin (OVA), CpG oligodeoxynucleotides (CpG OND), and cationic liposome (Lip) were taken as a model antigen, adjuvant, and microparticulate vehicle, respectively. Then, mice were immunized transcutaneously with dissolvable MNAs containing OVA, OVA-CpG OND, OVA encapsulated in Lip, OVA-CpG OND encapsulated in Lip and conventional IM injection with an OVA solution, respectively. They found that dissolvable MNAs containing OVA-CpG OND encapsulated in Lip had significantly higher amount of anti-OVA IgG antibody, and an increased level of IgG2a. MNAs containing OVA-CpG OND encapsulated in Lip also achieved the shift of immune type from predominate Th2 type to a balance Th1/Th2 type than that of the other groups.

5. CONCLUSION & FUTURE PROSPECTS

Microtechnologies offer new opportunities to develop miniaturized biocompatible devices for controlled drug delivery. Microtechnologies have the capability for the development of new controlled delivery systems and translate them into clinical practices by allowing one to explore the response and behavior of multiple tissues and organs in a highly integrated and defined way.

Multiple reservoir-based devices allow people to perform multiple drug delivery simultaneously with desired rates for each therapeutic. These microreservoirs can deliver both small and macromolecular therapeutics with specific targeting and control. Varieties of stimuli triggered controlled drug release system have been developed including pH, temperature, enzyme, and electro-magnetic fields. There is an increasing interest in drug delivery devices that can modulate the release of drug in response to some specific stimuli by different controlling approaches, which provides more options to selectively deliver therapeutic drugs in local cells or tissues according to different physiological environments and needs. Furthermore it is desired to exhibit low amounts

of leakage and easier to tune on-state release profiles in real time.

Microfabrication technology has enabled a variety of different MN designs for drug delivery to the skin and other targets depending upon the therapeutic drugs or the target site. Optimization of different parameters of MNs including sharpness, length, insertion force and velocity has also received extensive attention, which will assure more reliable MN insertion into the desired area and improve patient compliance and treatment. Several studies have shown that patients prefer MN-based delivery compared to hypodermic injections as they cause less pain and only cause mild transient erythema. The risk of infection at the target site was rarely reported. MNs have been studied for a range of medical applications, where delivery of bioactive substances to the skin has been the main focus.

Animal and human studies have demonstrated more efficient delivery of different therapeutic drugs and vaccines using microreservoir and microneedle-based systems. However, more efforts and research studies are needed to translate these encouraging technologies into effective, safe, and well controlled drug delivery for better clinical treatment and patient compliance. Microdevices should show long-term stability both outside and inside the body. The ideal drug delivery system also requires a monitored and triggered feedback to manage the drug release in response to a patient's body. We envision that microdevices will have great potential for a wide range of application in controlled drug delivery and release with distinct advantages over conventional drug delivery systems for effective personalized treatment, especially for effective cancer treatment with less side-effect.

CONFLICT OF INTEREST

All coauthors declare that they do not have any possible conflict of interest.

ACKNOWLEDGEMENTS

The Li group would like to acknowledge financial support of the National Institute of Allergy and Infectious Diseases of the National Institutes of Health (NIH) under award number R21AI107415, and the National Institute of General Medical Sciences of the NIH under award number SC2GM105584. Financial support from the IDR Program at the University of Texas at El Paso (UTEP) and the NIH RCMI Pilot Grant are also gratefully acknowledged.

REFERENCES

[1] Riahi, R.; Tamayol, A.; Shaegh, S.A.M.; Ghaemmaghami, A.M.; Dokmeci, M.R.; Khademshosseini, A. Microfluidics for advanced drug delivery systems. *Curr. Opin. Chem. Eng.,* **2015**, *7*, 101-112.

[2] Li, X.J.; Zhou, Y. Microfluidic devices for biomedical applications; Elsevier, 2013.

[3] Park, J.H.; Saravanakumar, G.; Kim, K.; Kwon, I.C. Targeted delivery of low molecular drugs using chitosan and its derivatives. *Adv. Drug Deliv. Rev.,* **2010**, *62*, 28-41.

[4] Bae, Y.H.; Park, K. Targeted drug delivery to tumors: myths, reality and possibility, *J. Control. Release,* **2011**, *153*, 198.

[5] Nguyen, N.-T.; Shaegh, S.A.M.; Kashaninejad, N.; Phan, D.-T. Design, fabrication and characterization of drug delivery systems based on lab-on-a-chip technology. *Adv. Drug Deliv. Rev.,* **2013**, *65*, 1403-1419.

[6] Sandri, G.; Bonferoni, M.C.; Ferrari, F.; Rossi, S.; Caramella, C.M. In *Particulate Products*; Springer, 2014, pp 323-341.

[7] Sethi, M.; Sukumar, R.; Karve, S.; Werner, M.E.; Wang, E.C.; Moore, D.T.; Kowalczyk, S.R.; Zhang, L.; Wang, A.Z. Effect of drug release kinetics on nanoparticle therapeutic efficacy and toxicity. *Nanoscale,* **2014**, *6*, 2321-2327.

[8] Kumar, K.S.; Bhowmik, D.; Srivastava, S.; Paswan, S.; Dutta, A. Sustained release drug delivery system potential. *Terminology,* **2012**, *1*, 2.

[9] Rajput, M.; Sharma, R.; Kumar, S.; Jamil, F.; Sissodia, N.; Sharma, S. Pulsatile drug delivery system: A review. *Int. J. Res. Pharmaceut. Biomed. Sci.,* **2012**, *3*, 118-124.

[10] Chiang, W.L.; Ke, C.J.; Liao, Z.X.; Chen, S.Y.; Chen, F.R.; Tsai, C.Y.; Xia, Y.; Sung, H.W. Pulsatile drug release from plga hollow microspheres by controlling the permeability of their walls with a magnetic field, *Small,* **2012**, *8*, 3584-3588.

[11] Jeon, G.; Yang, S.Y.; Byun, J.; Kim, J.K. Electrically actuatable smart nanoporous membrane for pulsatile drug release. *Nano lett.* **2011**, *11*, 1284-1288.

[12] Dou, M.; Dominguez, D.C.; Li, X.; Sanchez, J.; Scott, G. A versatile PDMS/paper hybrid microfluidic platform for sensitive infectious disease diagnosis, *Anal. Chem.,* **2014**, *86*, 7978-7986.

[13] Zuo, P.; Li, X.; Dominguez, D.C.; Ye, B.-C. A PDMS/paper/glass hybrid microfluidic biochip integrated with aptamer-functionalized graphene oxide nano-biosensors for one-step multiplexed pathogen detection, *Lab Chip,* **2013**, *13*, 3921-3928.

[14] Li, X.; Valadez, A. V.; Zuo, P.; Nie, Z. Microfluidic 3D cell culture: potential application for tissue-based bioassays, *Bioanalysis,* **2012**, *4*, 1509-1525.

[15] Liu, P.; Li, X.; Greenspoon, S.A.; Scherer, J.R.; Mathies, R.A. Integrated DNA purification, PCR, sample cleanup, and capillary electrophoresis microchip for forensic human identification, *Lab Chip,* **2011**, *11*, 1041-1048.

[16] Qi, H.; Huang, G.; Han, Y.L.; Lin, W.; Li, X.; Wang, S.; Lu, T.J.; Xu, F. *In vitro* spatially organizing the differentiation in individual multicellular stem cell aggregates, *Crit. Rev. Biotechnol.b* **2014**, 1-12.

[17] Xu, Q.; Hashimoto, M.; Dang, T.T.; Hoare, T.; Kohane, D.S.; Whitesides, G.M.; Langer, R.; Anderson, D.G. Preparation of monodisperse biodegradable polymer microparticles using a microfluidic flow-focusing device for controlled drug delivery, *Small,* **2009**, *5*, 1575-1581.

[18] Belliveau, N.M.; Huft, J.; Lin, P.J.; Chen, S.; Leung, A.K.; Leaver, T.J.; Wild, A.W.; Lee, J.B.; Taylor, R.J.; Tam, Y.K. Microfluidic synthesis of highly potent limit-size lipid nanoparticles for *in vivo* delivery of siRNA. *Molecul. Therap.-Nucleic Acids,* **2012**, *1*, e37.

[19] Brannon-Peppas, L.; Blanchette, J.O. Nanoparticle and targeted systems for cancer therapy. *Adv. Drug Deliv. Rev.,* **2012**, *64*, 206-212.

[20] Couvreur, P. Nanoparticles in drug delivery: Past, present and future. *Adv. Drug Deliv. Rev.,* **2013**, *65*, 21-23.

[21] Zhang, Y.; Chan, H.F.; Leong, K.W. Advanced materials and processing for drug delivery: The past and the future *Adv. Drug Deliv. Rev.* **2013**, *65*, 104-120.

[22] Mura, S.; Nicolas, J.; Couvreur, P. Stimuli-responsive nanocarriers for drug delivery. *Nature Mats,* **2013**, *12*, 991-1003.

[23] Nicolas, J.; Mura, S.; Brambilla, D.; Mackiewicz, N.; Couvreur, P. Design, functionalization strategies and biomedical applications of targeted biodegradable/biocompatible polymer-based nanocarriers for drug delivery. *Chem. Soc. Rev.,* **2013**, *42*, 1147-1235.

[24] Duncanson, W.J.; Lin, T.; Abate, A.R.; Seiffert, S.; Shah, R.K.; Weitz, D.A. Microfluidic synthesis of advanced microparticles for encapsulation and controlled release. *Lab Chip,* **2012**, *12*, 2135-2145.

[25] Neuži, P.; Giselbrecht, S.; Länge, K.; Huang, T.J.; Manz, A. Revisiting lab-on-a-chip technology for drug discovery. *Nat. Rev. Drug Discov.,* **2012**, *11*, 620-632.

[26] Sanjay, S.T.; Fu, G.; Dou, M.; Xu, F.; Liu, R.; Qi, H.; Li, X. Biomarker detection for disease diagnosis using cost-effective microfluidic platforms. *Analyst,* **2015**, *140*, 7062-7081.

[27] Dou, M.; Sanjay, S.T.; Benhabib, M.; Xu, F.; Li, X. Low-cost bioanalysis on paper-based and its hybrid microfluidic platforms. *Talanta,* **2015**.

[28] Liu, P.; Li, X.; Greenspoon, S.A.; Scherer, J.R.; Mathies, R.A. Integrated DNA purification, PCR, sample cleanup, and capillary

electrophoresis microchip for forensic human identification, *Lab Chip,* **2011**, *11*, 1041-1048.

[29] Mehta, G.; Hsiao, A.Y.; Ingram, M.; Luker, G.D.; Takayama, S. Opportunities and challenges for use of tumor spheroids as models to test drug delivery and efficacy, *J. Control. Release,* **2012**, *164*, 192-204.

[30] Balbino, T.A.; Aoki, N.T.; Gasperini, A.A.; Oliveira, C.L.; Azzoni, A.R.; Cavalcanti, L.P.; Lucimara, G. Continuous flow production of cationic liposomes at high lipid concentration in microfluidic devices for gene delivery applications. *Chem. Eng. J.,* **2013**, *226*, 423-433.

[31] DongáChung, T. Microfluidic approaches for gene delivery and gene therapy, *Lab Chip,* **2011**, *11*, 3941-3948.

[32] Shen, F.; Li, X.; Li, P.C. Study of flow behaviors on single-cell manipulation and shear stress reduction in microfluidic chips using computational fluid dynamics simulations, *Biomicrofluidics,* **2014**, *8*, 014109.

[33] Li, X.; Chen, Y.; Li, P.C. A simple and fast microfluidic approach of same-single-cell analysis (SASCA) for the study of multidrug resistance modulation in cancer cells, *Lab Chip,* **2011**, *11*, 1378-1384.

[34] Li, X.; Li, P.C. Strategies for the real-time detection of Ca^{2+} channel events of single cells: Recent advances and new possibilities, *Expert Rev. Clin. Pharmacol.,* **2010**, *3*.

[35] Witters, D.; Knez, K.; Ceyssens, F.; Puers, R.; Lammertyn, J. Digital microfluidics-enabled single-molecule detection by printing and sealing single magnetic beads in femtoliter droplets. *Lab Chip,* **2013**, *13*, 2047-2054.

[36] Ashraf, M.W.; Tayyaba, S.; Afzulpurkar, N. Micro electromechanical systems (MEMS) based microfluidic devices for biomedical applications, *Int. J. Mol. Sci.,* **2011**, *12*, 3648-3704.

[37] Staples, M.; Daniel, K.; Cima, M.J.; Langer, R. Application of micro-and nano-electromechanical devices to drug delivery, *Pharmaceut. Res.,* **2006**, *23*, 847-863.

[38] Stępak, B.; Antończak, A.; Bartkowiak-Jowsa, M.; Filipiak, J.; Pezowicz, C.; Abramski, K. Fabrication of a polymer-based biodegradable stent using a CO 2 laser. *Archiv. Civil Mechanic. Engin.,* **2014**, *14*, 317-326.

[39] Lu, Y.; Chen, S. Micro and nano-fabrication of biodegradable polymers for drug delivery. *Adv. Drug Deliv. Rev.,* **2004**, *56*, 1621-1633.

[40] Criales, L.E.; Orozco, P.F.; Medrano, A.; Rodríguez, C.A.; Özel, T. Effect of fluence and pulse overlapping on fabrication of microchannels in PMMA/PDMS Via UV Laser micromachining: Modeling and experimentation. *Mat. Manufactur. Proc.,* **2015**, 1-12.

[41] Malinauskas, M.; Juodkazis, S. In *Fundamentals of Laser-Assisted Micro-and Nanotechnologies*; Springer, 2014, pp 271-291.

[42] Indermun, S.; Luttge, R.; Choonara, Y.E.; Kumar, P.; du Toit, L.C.; Modi, G.; Pillay, V. Current advances in the fabrication of microneedles for transdermal delivery. *J. Control. Release* **2014**, *185*, 130-138.

[43] Kim, Y.-C.; Park, J.-H.; Prausnitz, M.R. Microneedles for drug and vaccine delivery. *Adv. Drug Deliv. Rev.,* **2012**, *64*, 1547-1568.

[44] Ochoa, M.; Mousoulis, C.; Ziaie, B. Polymeric microdevices for transdermal and subcutaneous drug delivery. *Adv. Drug Deliv. Rev.,* **2012**, *64*, 1603-1616.

[45] Kim, J.D.; Kim, M.; Yang, H.; Lee, K.; Jung, H. Droplet-born air blowing: Novel dissolving microneedle fabrication. *J. Control. Release,* **2013**, *170*, 430-436.

[46] Lee, K.; Lee, C.Y.; Jung, H. Dissolving microneedles for transdermal drug administration prepared by stepwise controlled drawing of maltose. *Biomaterials,* **2011**, *32*, 3134-3140.

[47] Stevenson, C.L.; Santini, J.T.; Langer, R. Reservoir-based drug delivery systems utilizing microtechnology. *Adv. Drug Deliv. Rev.,* **2012**, *64*, 1590-1602.

[48] Pan, L.; He, Q.; Liu, J.; Chen, Y.; Ma, M.; Zhang, L.; Shi, J. Nuclear-targeted drug delivery of TAT peptide-conjugated monodisperse mesoporous silica nanoparticles. *J. Am. Chem. Soc.,* **2012**, *134*, 5722-5725.

[49] Oliveira, H.; Pérez-Andrés, E.; Thevenot, J.; Sandre, O.; Berra, E.; Lecommandoux, S. Magnetic field triggered drug release from polymersomes for cancer therapeutics. *J. Control. Release,* **2013**, *169*, 165-170.

[50] Anglin, E.J.; Cheng, L.; Freeman, W.R.; Sailor, M.J. Porous silicon in drug delivery devices and materials. *Adv. Drug Deliv. Rev.,* **2008**, *60*, 1266-1277.

[51] Hernandez-Montelongo, J.; Naveas, N.; Degoutin, S.; Tabary, N.; Chai, F.; Spampinato, V.; Ceccone, G.; Rossi, F.; Torres-Costa, V.; Manso-Silvan, M. Porous silicon-cyclodextrin based polymer composites for drug delivery applications. *Carbohyd. Polym.,* **2014**, *110*, 238-252.

[52] Masi, B.C.; Tyler, B.M.; Bow, H.; Wicks, R.T.; Xue, Y.; Brem, H.; Langer, R.; Cima, M.J. Intracranial MEMS based temozolomide delivery in a 9L rat gliosarcoma model, *Biomaterials,* **2012**, *33*, 5768-5775.

[53] Pirmoradi, F.N.; Jackson, J.K.; Burt, H.M.; Chiao, M. On-demand controlled release of docetaxel from a battery-less MEMS drug delivery device. *Lab Chip,* **2011**, *11*, 2744-2752.

[54] McInnes, S.J.; Szili, E.J.; Al-Bataineh, S.A.; Xu, J.; Alf, M.E.; Gleason, K.K.; Short, R.D.; Voelcker, N.H. Combination of iCVD and porous silicon for the development of a controlled drug delivery system. *ACS Appl. Mater. Iinterfac.,* **2012**, *4*, 3566-3574.

[55] Elman, N.; Masi, B.; Cima, M.; Langer, R. Electro-thermally induced structural failure actuator (ETISFA) for implantable controlled drug delivery devices based on Micro-Electro-Mechanical-Systems, *Lab Chip,* **2010**, *10*, 2796-2804.

[56] Gensler, H.; Sheybani, R.; Li, P.-Y.; Mann, R.L.; Meng, E. An implantable MEMS micropump system for drug delivery in small animals, *Biomedic. Microdevices,* **2012**, *14*, 483-496.

[57] Farra, R.; Sheppard, N.F.; McCabe, L.; Neer, R.M.; Anderson, J.M.; Santini, J.T.; Cima, M.J.; Langer, R. First-in-human testing of a wirelessly controlled drug delivery microchip. *Sci. Translation. Med.,* **2012**, *4*, 122ra121-122ra121.

[58] Petersen, R.S.; Keller, S.S.; Boisen, A. Hot punching of high-aspect-ratio 3D polymeric microstructures for drug delivery, *Lab Chip,* **2015**, *15, 2576*.

[59] Timko, B.P.; Arruebo, M.; Shankarappa, S.A.; McAlvin, J.B.; Okonkwo, O.S.; Mizrahi, B.; Stefanescu, C.F.; Gomez, L.; Zhu, J.; Zhu, A. Near-infrared–actuated devices for remotely controlled drug delivery, *Proc. Natl. Acad. Sci.,* **2014**, *111*, 1349-1354.

[60] Zaman, R.T.; Gopal, A.; Starr, K.; Zhang, X.; Thomsen, S.; Tunnell, J.W.; Welch, A.J.; Rylander, H.G. Micro-patterned drug delivery device for light-activated drug release. *Lasers Surg. Med.,* **2012**, *44*, 30-48.

[61] Tobias, I.S.; Lee, H.; Engelmayr, G.C.; Macaya, D.; Bettinger, C.J.; Cima, M.J. Zero-order controlled release of ciprofloxacin-HCl from a reservoir-based, bioresorbable and elastomeric device. *J. Control. Release,* **2010**, *146*, 356-362.

[62] Chirra, H.D.; Desai, T.A. Multi-reservoir bioadhesive microdevices for independent rate-controlled delivery of multiple drugs. *Small,* **2012**, *8*, 3839-3846.

[63] Tuan-Mahmood, T.-M.; McCrudden, M.T.; Torrisi, B.M.; McAlister, E.; Garland, M.J.; Singh, T.R.R.; Donnelly, R.F. Microneedles for intradermal and transdermal drug delivery. *Eur. J. Pharm. Sci.,* **2013**, *50*, 623-637.

[64] van der Maaden, K.; Jiskoot, W.; Bouwstra, J. Microneedle technologies for (trans) dermal drug and vaccine delivery. *J. Control. Release* **2012**, *161*, 645-655.

[65] RR Singh, T.; J Dunne, N.; Cunningham, E.; F Donnelly, R. Review of patents on microneedle applicators. *Rec. Pat. Drug Deliv. Formul.,* **2011**, *5*, 11-23.

[66] Norman, J.J.; Arya, J.M.; McClain, M.A.; Frew, P.M.; Meltzer, M.I.; Prausnitz, M.R. Microneedle patches: Usability and acceptability for self-vaccination against influenza. *Vaccine,* **2014**, *32*, 1856-1862.

[67] Coleman, B.L.; McGeer, A.J.; Halperin, S.A.; Langley, J.M.; Shamout, Y.; Taddio, A.; Shah, V.; McNeil, S.A.A randomized control trial comparing immunogenicity, safety, and preference for self-versus nurse-administered intradermal influenza vaccine. *Vaccine,* **2012**, *30*, 6287-6293.

[68] Bystrova, S.; Luttge, R. Micromolding for ceramic microneedle arrays. *Microelectron. Engin.,* **2011**, *88*, 1681-1684.

[69] Donnelly, R.F.; Majithiya, R.; Singh, T.R.R.; Morrow, D.I.; Garland, M.J.; Demir, Y.K.; Migalska, K.; Ryan, E.; Gillen, D.; Scott, C.J. Design, optimization and characterisation of polymeric microneedle arrays prepared by a novel laser-based micromoulding technique. *Pharmaceut. Res.,* **2011**, *28*, 41-57.

[70] Römgens, A.; Bader, D.; Bouwstra, J.; Baaijens, F.; Oomens, C. Monitoring the penetration process of single microneedles with varying tip diameters. *J. Mech. Behav. Biomed.,* **2014**, *40*, 397-405.

[71] Traverso, G.; Schoellhammer, C.M.; Schroeder, A.; Maa, R.; Lauwers, G.Y.; Polat, B.E.; Anderson, D.G.; Blankschtein, D.; Langer, R. Microneedles for drug delivery via the gastrointestinal tract. *J. Pharmaceut. Sci.,* **2015**, *104*, 362-367.

[72] Kaur, M.; Ita, K.B.; Popova, I.E.; Parikh, S.J.; Bair, D.A. Microneedle-assisted delivery of verapamil hydrochloride and amlodipine besylate. *Eur. J. Pharm. Biopharm.,* **2014**, *86*, 284-291.

[73] Kumar, A.; Li, X.; Sandoval, M.A.; Rodriguez, B.L.; Sloat, B.R.; Cui, Z. Permeation of antigen protein-conjugated nanoparticles and live bacteria through microneedle-treated mouse skin. *Int. J. Nanomed.,* **2011**, *6*, 1253-1264.

[74] Zhang, S.; Qiu, Y.; Gao, Y. Enhanced delivery of hydrophilic peptides *in vitro* by transdermal microneedle pretreatment, *Acta Pharmaceutica Sinica, B* **2014**, *4*, 100-104.

[75] Vinayakumar, K.B.; Hegde, G.M.; Ramachandra, S.G.; Nayak, M.M.; Dinesh, N.S.; Rajanna, K. Development of cup shaped microneedle array for transdermal drug delivery. *Biointerphases,* **2015**, *10*, 021008.

[76] van der Maaden, K.; Sekerdag, E.; Schipper, P.; Kersten, G.; Jiskoot, W.; Bouwstra, J. Layer-by-layer assembly of inactivated poliovirus and N-trimethyl chitosan on pH-sensitive microneedles for dermal vaccination, *Langmuir,* **2015**, *31*, 8654-8660.

[77] Witting, M.; Obst, K.; Pietzsch, M.; Friess, W.; Hedtrich, S. Feasibility study for intraepidermal delivery of proteins using a solid microneedle array. *Int. J. Pharm.,***2015**, *486*, 52-58.

[78] Pearton, M.; Saller, V.; Coulman, S.A.; Gateley, C.; Anstey, A.V.; Zarnitsyn, V.; Birchall, J.C. Microneedle delivery of plasmid DNA to living human skin: formulation coating, skin insertion and gene expression. *J. Control. Release,* **2012**, *160*, 561-569.

[79] Ma, Y.; Boese, S.E.; Luo, Z.; Nitin, N.; Gill, H.S. Drug coated microneedles for minimally-invasive treatment of oral carcinomas: development and *in vitro* evaluation. *Biomedic. Microdevices,* **2015**, *17*, 1-14.

[80] Kim, Y.C.; Edelhauser, H.F.; Prausnitz, M.R. Intracorneal delivery of bevacizumab using microneedles to treat injury-induced neovascularization. *Invest. Ophthalmol. Vis. Sci.,* **2012**, *53*, 507-507.

[81] Zhang, Y.; Brown, K.; Siebenaler, K.; Determan, A.; Dohmeier, D.; Hansen, K. Development of lidocaine-coated microneedle product for rapid, safe, and prolonged local analgesic action. *Pharmaceut. Res.,* **2012**, *29*, 170-177.

[82] Choi, H.-J.; Yoo, D.-G.; Bondy, B.J.; Quan, F.-S.; Compans, R.W.; Kang, S.-M.; Prausnitz, M.R. Stability of influenza vaccine coated onto microneedles. *Biomaterials,* **2012**, *33*, 3756-3769.

[83] Weldon, W.C.; Zarnitsyn, V.G.; Esser, E.S.; Taherbhai, M.T.; Koutsonanos, D.G.; Vassilieva, E.V.; Skountzou, I.; Prausnitz, M.R.; Compans, R.W. Effect of adjuvants on responses to skin immunization by microneedles coated with influenza subunit vaccine. *PloS One,* **2012**, *7*, e41501.

[84] Ma, Y.; Tao, W.; Krebs, S.J.; Sutton, W.F.; Haigwood, N.L.; Gill, H.S. Vaccine delivery to the oral cavity using coated microneedles induces systemic and mucosal immunity. *Pharmaceut. Res.,* **2014**, *31*, 2393-2403.

[85] Jun, H.; Han, M.-R.; Kang, N.-G.; Park, J.-H.; Park, J.H. Use of hollow microneedles for targeted delivery of phenylephrine to treat fecal incontinence. *J. Control. Release,* **2015**, *207*, 1-6.

[86] Patel, S.R.; Lin, A.S.; Edelhauser, H.F.; Prausnitz, M.R. Suprachoroidal drug delivery to the back of the eye using hollow microneedles. *Pharmaceut. Res.,* **2011**, *28*, 166-176.

[87] Lyon, B.J.; Aria, A.I.; Gharib, M. Fabrication of carbon nanotube-polyimide composite hollow microneedles for transdermal drug delivery. *Biomed. Microdevices,* **2014**, *16*, 879-886.

[88] Norman, J.J.; Brown, M.R.; Raviele, N.A.; Prausnitz, M.R.; Felner, E.I. Faster pharmacokinetics and increased patient acceptance of intradermal insulin delivery using a single hollow microneedle in children and adolescents with type 1 diabetes, *Pediatric Diabet.,* **2013**, *14*, 459-465.

[89] van der Maaden, K.; Trietsch, S.J.; Kraan, H.; Varypataki, E.M.; Romeijn, S.; Zwier, R.; van der Linden, H.J.; Kersten, G.; Hankemeier, T.; Jiskoot, W. Novel hollow microneedle technology for depth-controlled microinjection-mediated dermal vaccination: a study with polio vaccine in rats. *Pharmaceut. Res.,* **2014**, *31*, 1846-1854.

[90] van der Maaden, K.; Luttge, R.; Vos, P.J.; Bouwstra, J.; Kersten, G.; Ploemen, I. Microneedle-based drug and vaccine delivery via nanoporous microneedle arrays, *Drug Deliv. Transl. Res.,* **2015**, 1-10.

[91] Verhoeven, M.; Bystrova, S.; Winnubst, L.; Qureshi, H.; De Gruijl, T. D.; Scheper, R. J.; Luttge, R. Applying ceramic nanoporous microneedle arrays as a transport interface in egg plants and an *ex-vivo* human skin model. *Microelectron. Engin.,* **2012**, *98*, 659-662.

[92] Yan, X.-X.; Liu, J.-Q.; Jiang, S.-D.; Yang, B.; Yang, C.-S. Fabrication and testing of porous Ti microneedles for drug delivery. *Micro & Nano Lett., IET* **2013**, *8*, 906-908.

[93] Kochhar, J.S.; Lim, W. X.S.; Zou, S.; Foo, W.Y.; Pan, J.; Kang, L. Microneedle integrated transdermal patch for fast onset and sustained delivery of lidocaine, *Molecul. Pharmaceut.,* **2013**, *10*, 4272-4280.

[94] Donnelly, R.F.; Singh, T.R.R.; Woolfson, A.D. Microneedle-based drug delivery systems: Microfabrication, drug delivery, and safety. *Drug Deliv.,* **2010**, *17*, 187-207.

[95] Martin, C.; Allender, C.J.; Brain, K.R.; Morrissey, A.; Birchall, J.C. Low temperature fabrication of biodegradable sugar glass microneedles for transdermal drug delivery applications. *J. Control. Release,* **2012**, *158*, 93-101.

[96] Lee, J.W.; Choi, S.O.; Felner, E.I.; Prausnitz, M.R. Dissolving microneedle patch for transdermal delivery of human growth hormone. *Small*, **2011**, *7*, 531-539.

[97] Cha, K.J.; Kim, T.; Park, S.J.; Kim, D.S. Simple and cost-effective fabrication of solid biodegradable polymer microneedle arrays with adjustable aspect ratio for transdermal drug delivery using acupuncture microneedles. *J. Micromechanics Microengin.,* **2014**, *24*, 115015.

[98] Garland, M.J.; Caffarel–Salvador, E.; Migalska, K.; Woolfson, A.D.; Donnelly, R.F. Dissolving polymeric microneedle arrays for electrically assisted transdermal drug delivery. *J. Control. Release,* **2012**, *159*, 52-59.

[99] Liu, S.; Jin, M.-N.; Quan, Y.-S.; Kamiyama, F.; Kusamori, K.; Katsumi, H.; Sakane, T.; Yamamoto, A. Transdermal delivery of relatively high molecular weight drugs using novel self-dissolving microneedle arrays fabricated from hyaluronic acid and their characteristics and safety after application to the skin. *Eur. J. Pharm. Biopharm.,* **2014**, *86*, 267-276.

[100] Sullivan, S.P.; Koutsonanos, D.G.; del Pilar Martin, M.; Lee, J.W.; Zarnitsyn, V.; Choi, S.-O.; Murthy, N.; Compans, R. W.; Skountzou, I.; Prausnitz, M.R. Dissolving polymer microneedle patches for influenza vaccination. *Nat. Med.,* **2010**, *16*, 915-920.

[101] Guo, L.; Chen, J.; Qiu, Y.; Zhang, S.; Xu, B.; Gao, Y. Enhanced transcutaneous immunization via dissolving microneedle array loaded with liposome encapsulated antigen and adjuvant. *Int. J. Pharmaceut.,* **2013**, *447*, 22-30.

Received: November 23, 2015 Revised: January 21, 2016 Accepted: January 21, 2016